



Influence of microstructure on near-threshold fatigue crack growth behavior of 18Ni maraging steel weldment

Haitao Zhao^{1,2} · Delun Guo² · Qi Qin¹ · Sujun Wu¹

Received: 22 September 2022 / Accepted: 4 September 2023 / Published online: 20 September 2023
© International Institute of Welding 2023

Abstract

The influence of microstructure of weld metal on near-threshold crack growth behavior under the condition of low and high stress ratio has not been deeply understood. Therefore, experiments were carried out to study the influence of microstructure on the near-threshold fatigue crack growth behavior of 18Ni maraging steel and weld. Microstructure characteristics of base metal and weld metal were analyzed by optical microscope and scanning electron microscope. Results show that the segregation of elements such as Mo, Ti, and Ni leads to the formation of massive reversed austenite phases in the weld interdendritic region and correspondingly reduces the content of these elements in martensite matrix of weld metal, thereby reducing the amount of N_3 (Mo, Ti) in the weld matrix, leading to decrease of microhardness and tensile strength of weld metal compared to that of base metal. Fatigue tests demonstrate that when the stress ratio is 0.1 and fatigue crack growth rate is less than 10^{-5} mm/cycle, roughness-induced crack closure effect has a great influence on crack growth behavior of base metal. The near-threshold crack growth rate of weld metal is lower than that of base metal under the stress ratio of 0.9, which can be attributed to the larger average size of martensite blocks and lower density of high-angle boundaries in weld metal than in base metal.

Keywords Near-threshold fatigue crack growth · Weld metal · Base metal · Martensite block · Microstructure

1 Introduction

Defects or damages inevitably appear in metal structures during engineering manufacture and during service, where fatigue cracks often occur and extend to structure failure under cyclic loading. Therefore, researches on fatigue crack growth behavior have become an important part of structural durability analysis. Many researches [1–4] have found that microstructure characteristics have significant influence on near-threshold crack growth behavior with low stress intensity amplitude ΔK , which is related to roughness-induced crack

closure. Sun et al. [5] revealed that grain size of prior austenite in martensitic steel was proportional to roughness of crack growth path section, and large grain size increased roughness-induced crack closure effect, which led to the decreasing of near-threshold fatigue crack growth rate. Gary et al. [6] suggested that in eutectoid steel, near-threshold crack growth path depended on the orientation of pearlite beam, which affected roughness-induced crack closure effect and final fatigue crack growth rate and threshold value. Recently, SunLingen [7] also revealed that heterogeneous grain size of prior austenite in the weld metal of refractory steel has an obvious influence on near-threshold crack growth behavior, and the difference of crack closure effect caused by heterogeneous grain size makes the test data of crack growth rate show great dispersion. Additionally, it has been found that the effect of load ratio R which is defined as ratio of minimum to maximum load ($R = P_{\min}/P_{\max}$) on crack growth behavior also depends on microstructures [8–11]. In a metastable beta titanium alloy, Jha and Ravichandran [12] found that stress ratio had a negligible effect on crack growth behavior of the α -aged microstructure, while a strong effect was observed in the ω -aged microstructure due to its higher level of roughness-induced crack closure.

Recommended for publication by Commission XI - Pressure Vessels, Boilers, and Pipelines

✉ Sujun Wu
wusj@buaa.edu.cn

¹ School of Material Science and Engineering, Beihang University, Beijing, China

² Aeronautical Key Laboratory for Welding and Joining Technologies, AVIC Manufacturing Technology Institute, Beijing, China

Martensite steel material has been applied to various kinds of aviation welded structures. During the service period of structures, fatigue cracks usually occur at the weldment and extend to the structure failure. Ming Yang [13] analyzed systematically the influence of microstructure of prior austenite grain, martensite packet, and martensite block in martensite steel on fatigue crack growth resistance and pointed out that when the size of cyclic plastic zone is equal to or more than the average size of martensite block, the first significant transition point occurs, and the smallest plastic deformation unit at the crack tip changes from martensite lath to martensite block. When the size of cyclic plastic zone reaches the average size of martensite packet, the plastic deformation unit changes from martensite block to martensite package again, which leads to the second transition point of fatigue crack growth behavior. However, what role does the microstructure of martensite steel does play during near-threshold crack growth without crack closure effect? Especially, the effect of microstructure of weld metal on near-threshold crack growth behavior has not been deeply understood. In this paper, microstructure characteristics and basic mechanical properties of weld metal of 18Ni maraging steel were analyzed, and the mechanism of the influence of microstructure characteristics on near-threshold fatigue crack growth behavior was discussed.

2 Experimental materials and methods

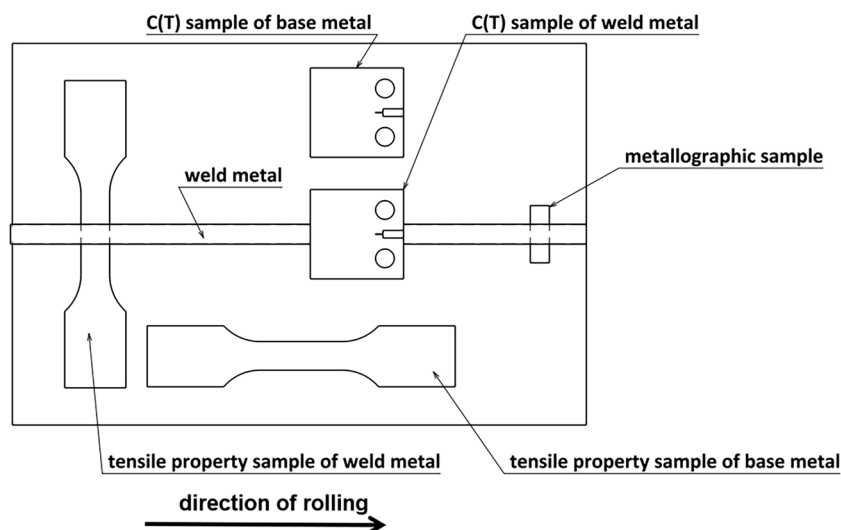
The material used in the experiment is 18Ni maraging steel, which is a kind of super-strength steel with ultra-low carbon and Fe–Ni martensite matrix. As-forged, major chemical components are shown in Table 1. The welded specimens were prepared by argon tungsten arc welding method. That is, firstly, the first pass was welded on the front side, and then the second pass was welded on the back side to manufacture welded specimen. Welded specimens were put into a vacuum furnace for solution treatment and subsequent aging treatment. The parameters of solution treatment are as follows: holding at 830 °C for 1.5 h and air cooling, in order to obtain Fe–Ni martensite matrix; the aging parameters are as follows: holding at 480 °C for 4.5 h and air cooling, in order to precipitate dispersedly strengthening phases of Ni₃ (Mo, Ti) in martensite matrix.

Metallographic samples composed of weld metal, heat-affected zone (HAZ), and base metal were taken from welded specimens, as shown in Fig. 1. After polishing observation surface of metallographic samples, microstructure and morphology were etched out with 4% nitric acid alcohol solution. Microstructure characteristics of weld metal, HAZ, and base metal were observed by Leica DM5000 optical metallographic microscope (OM) and JSM-7900F scanning

Table 1 Major chemical components of 18Ni maraging steel (wt%)

| C | Ni | Mo | Co | Cr | Si | Ti | Al | Mn | Si | Cu | Fe |
|-------|-------------|-----------|-----------|------|-------|-----------|-----------|-------|------|------|---------|
| ≤0.02 | 17.50~19.00 | 4.60~5.20 | 7.50~8.50 | ≤0.5 | ≤0.10 | 0.30~0.50 | 0.05~0.15 | ≤0.10 | 0.14 | ≤0.5 | balance |

Fig. 1 Schematic diagram of sampling position of mechanical sample and metallographic sample of weld metal and base metal



electron microscope (SEM), respectively. Element contents of major phases were analyzed by energy spectrum method, and micro-grain orientation maps were analyzed by selected area electron backscattering diffraction (EBSD). Microhardness of metallographic samples was measured by FM800 micro Vickers hardness tester.

Tensile property samples of both weld metal and base metal were taken from welded specimens, as shown in Fig. 1. Room temperature tensile properties were tested on an EMSYS tensile testing machine. C(T) samples required for the fatigue crack growth rate test of both weld metal and base metal also were taken, as shown in Fig. 1. The dimension of C(T) sample is shown in Fig. 2. Especially, for C(T) samples of weld metal, fatigue crack was prepared at the middle position of weld metal. The fatigue crack growth behavior of both weld metal and base metal was tested on MTS Landmark Fatigue Testing Machine. Firstly, near-threshold fatigue crack growth rate with less than 10^{-5} mm/cycle was tested by gradually decreasing K method under the condition of constant stress ratio R . Then, fatigue crack growth rate in the Paris region with more than 10^{-5} mm/cycle was tested under the condition of constant stress ratio R by the method of increasing K under constant load.

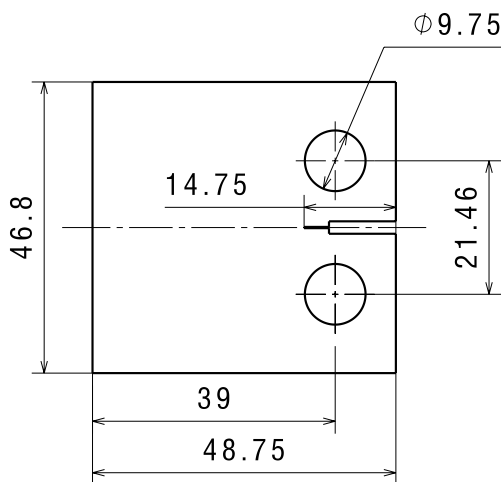
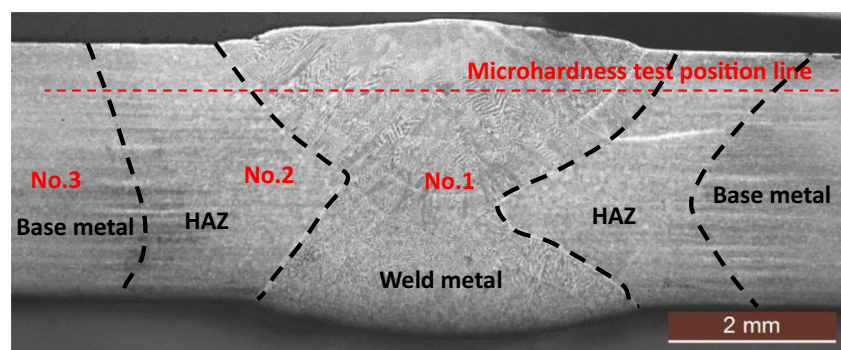


Fig. 2 Major dimensions of C(T) sample with thickness of 2.5 mm

Fig. 3 Macro-morphology of weldment of 18Ni maraging steel



Equation (1) was used to calculate the magnitude of stress intensity factor. The morphology of the crack growth path was observed with a Leica DM5000 optical metallographic microscope.

$$\Delta K = \frac{\Delta P}{B\sqrt{W}} \frac{(2 + \alpha)}{(1 - \alpha)^{\frac{3}{2}}} (0.886 + 4.64\alpha - 13.32\alpha^2 + 14.72\alpha^3 - 5.6\alpha^4) \quad (1)$$

Among them, $\alpha = a/W$; a is crack length, B is thickness of C(T) sample, W is width of C(T) sample, and ΔP is applied load amplitude. Linear fitting calculation method was used to deal with the data of fatigue crack growth rate.

3 Results

3.1 Microstructure characteristics

The 18Ni weldment consists of weld metal, heat affected zone, and base metal, as shown in Fig. 3. During the welding process, base metal is not affected by welding heat, and its microstructure characteristics are consistent with original material with prior austenite grains of about $28.2 \mu\text{m}$ size and fine lath martensite phases in the matrix, as shown in Fig. 4a. Weld metal is the microstructure of dendritic casting structure formed by melting and subsequent solidification of metal materials with the average width of dendrites of about $16 \mu\text{m}$, as shown in the Fig. 4c. Fine lath martensite precipitates inside dendrites of weld metal with reversed austenite phases in the interdendrites, as indicated by arrows in Fig. 5c. Heat-affected zone is located between weld metal and base metal with coarse prior austenite grain of average about $71.5 \mu\text{m}$ near weld fusion line, as shown in Fig. 4b.

As we all know, welding solidification process is often accompanied by the phenomenon that some elements segregate into interdendrites. There is a serious segregation of Mo, Ti, and Ni elements into the interdendrites of 18Ni weld metal, as shown in Fig. 5. Correspondingly, the contents of these elements in martensite matrix will inevitably decrease. Since these elements are the major elements of precipitation strengthening phases Ni_3 (Mo, Ti), the number of

Fig. 4 Microstructure and morphology of weldment of 18Ni maraging steel

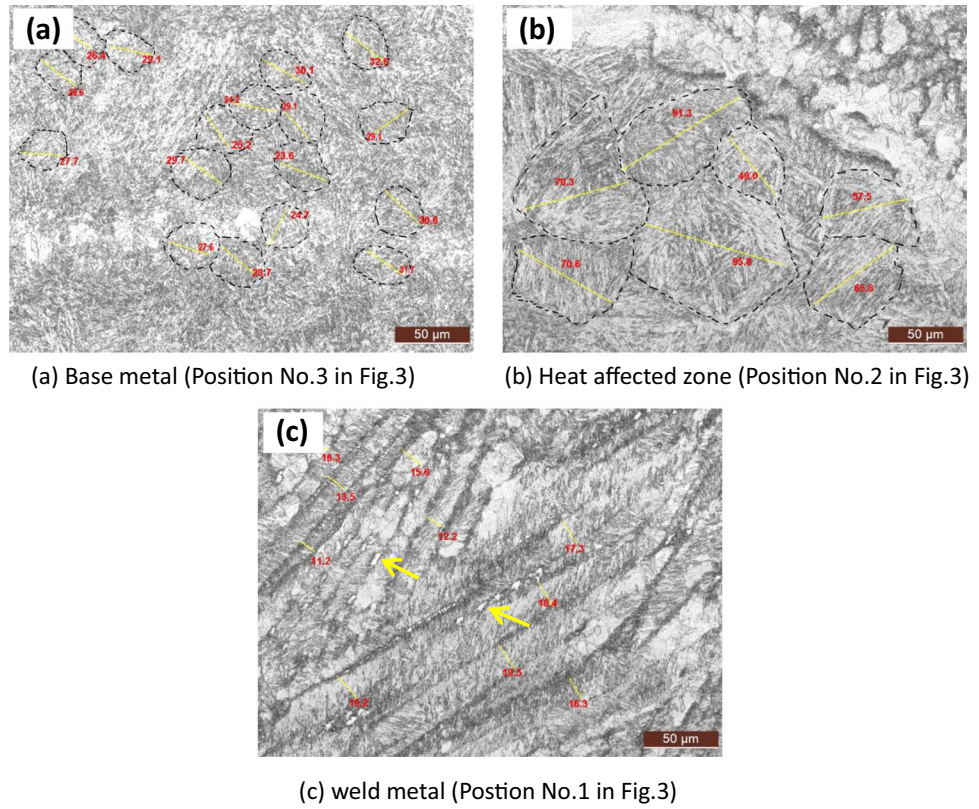
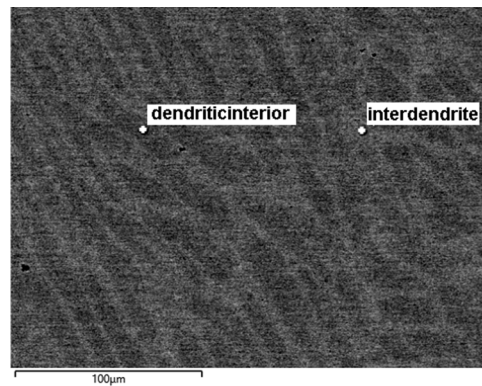


Fig. 5 Energy spectrum analysis results of main elements in weld metal



| Test position | Ni | Mo | Co | Ti | Fe |
|--------------------|-------|------|------|------|-------|
| interdendrite | 19.34 | 1.30 | 8.39 | 0.79 | 70.18 |
| dendritic interior | 17.51 | 0.05 | 8.37 | 0.31 | 73.76 |

Noting: the atomic percentage is calculated after minor elements are not included.

precipitation strengthening phases in the martensite matrix is expected to decrease accordingly. During the aging treatment, the strengthening phases such as Ni₃(Ti, Mo) are precipitated dispersedly along the martensite phase boundaries in the form of fine particles, as shown in Fig. 6. This precipitation strength mechanism generally contributes about 1000~2000 MPa to the kind of maraging steel [9–14].

As pointed out in Reference, [14–16] since Fe–Ni martensite is metastable during the aging process, austenite phase reverse reaction tends to occur in the Mo, Ti, and Ni enriched regions of interdendrites where massive reversed austenite phases are formed, as indicated by the arrows in Fig. 4c. The phase amount of weld metal and base metal analyzed by EBSD method is shown in Fig. 7. The matrix

Fig. 6 Morphology of strengthening phases precipitated dispersedly along lath martensite phase boundaries

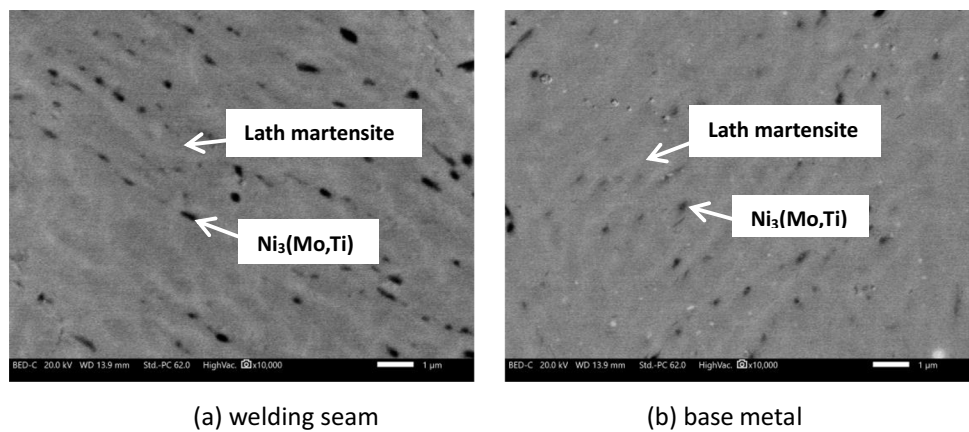
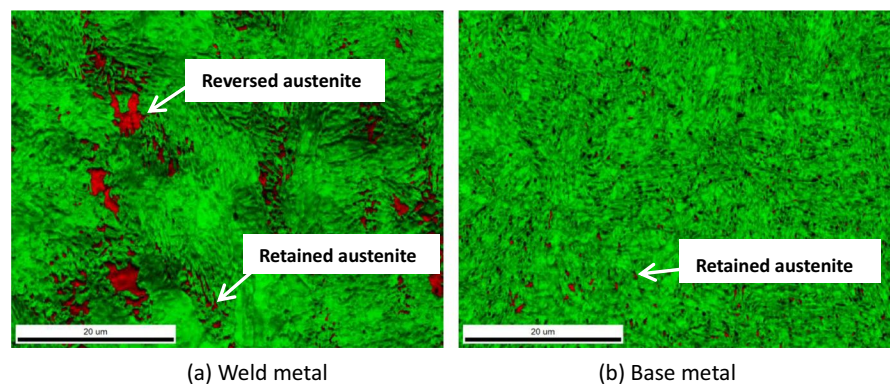


Fig. 7 EBSD test results of phase content in weld metal and base metal of 18Ni maraging steel



| Phase type (ratio by volume) | Weld metal | Base metal |
|------------------------------|------------|------------|
| Austenite phase (red) | 0.068 | 0.012 |
| Martensite phase (green) | 0.932 | 0.988 |

structures of them are both lath martensite phases, with a small amount of retained austenite phases distributed along lath martensite phase boundaries. It is also worth noting that there are general and massive reversed austenite phases in the interdendrites of weld metal. Statistical results showed that the total amount of retained austenite phase and reversed austenite phase in weld metal was 5 times more than that in base metal. Consequently, formation of austenite phase consumes more elements such as Mo, Ti, and Ni in weld metal, which will be expected to accordingly lead to decrease the number of precipitation strengthening phases in the martensite matrix, which will inevitably have negative influences on the number of precipitation strengthening phase such as $Ni_3(Mo, Ti)$ in the matrix, thus affecting mechanical properties of weld metal [17].

3.2 Microhardness and tensile properties

The microhardness of 18Ni maraging steel weldment was tested along the dotted line shown in Fig. 3, and the distance between adjacent test points is 0.2 mm. Figure 8 shows the

result of microhardness distribution in the weldment. The microhardness value of base metal was the highest, with the average value of about $592.2 HV_{0.3}$, and the “valley” of the microhardness distribution appeared in the central position of weld metal, where the average value of microhardness was about $552.7 HV_{0.3}$. Obviously, the reason for this phenomenon should be directly relative to the abovementioned segregation of Ni, Mo, and Ti in weld metal, which reduced the number of precipitation strengthening phases $Ni_3(Mo, Ti)$ in the matrix [13, 14] while the results of room temperature tensile test further proved that the tensile strength and yield strength of weld metal were lower than that of base metal, as shown in Table 2.

3.3 Fatigue crack growth behavior

Figure 9 shows the test results of fatigue crack growth behavior of both weld metal and base metal under the condition of stress ratio value of 0.1, 0.5, and 0.9, respectively. The fatigue crack growth rate of both materials increased with the increase of stress ratio. At the stage of fatigue

Fig. 8 Distribution of micro-hardness of weldment of 18Ni maraging steel

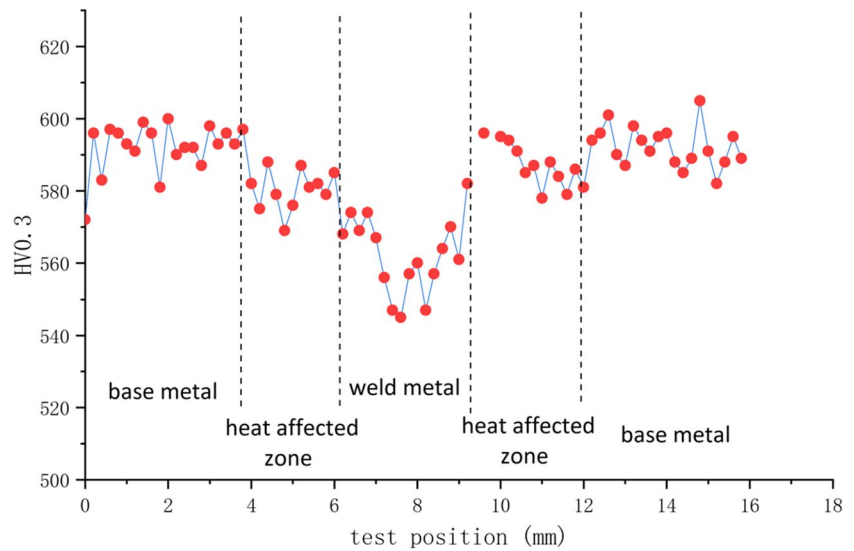


Table 2 Test results of tensile properties of 18Ni maraging steel and weldment in room temperature

| Sample type | Rm (MPa) | Rp0.2 (MPa) | A (%) | Fracture position |
|-------------|----------|-------------|-------|-------------------|
| Base metal | 1887.4 | 1870.6 | 7.24 | Base metal |
| Weld metal | 1826 | 1744.6 | 6.4 | Weld metal |

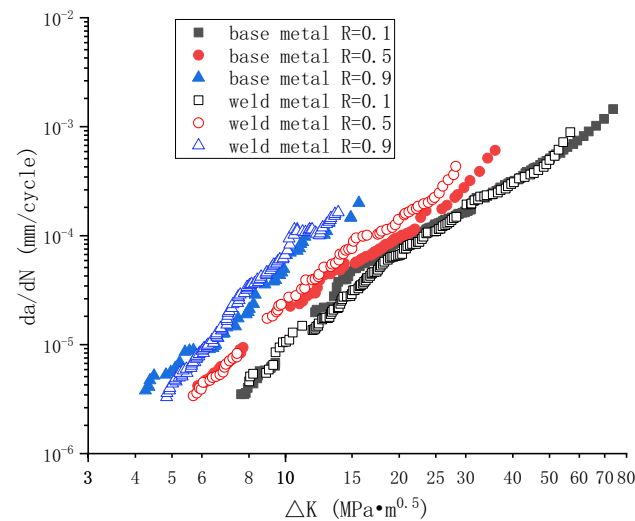


Fig. 9 Fatigue crack growth rate curves under the conditions of different stress ratios

crack growth rate between 10^{-5} and 10^{-4} mm/cycle, corresponding to large ΔK -values, the fatigue crack growth rates of both materials were almost the same under the same stress ratio, which reflected the conclusion of Reference [6, 18], that is, microstructure has little influence on fatigue crack growth behavior under the condition of large ΔK -values. However, at the near-threshold stage of fatigue

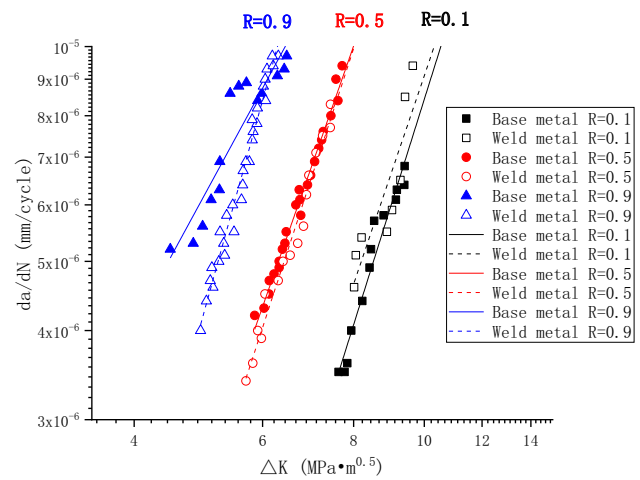
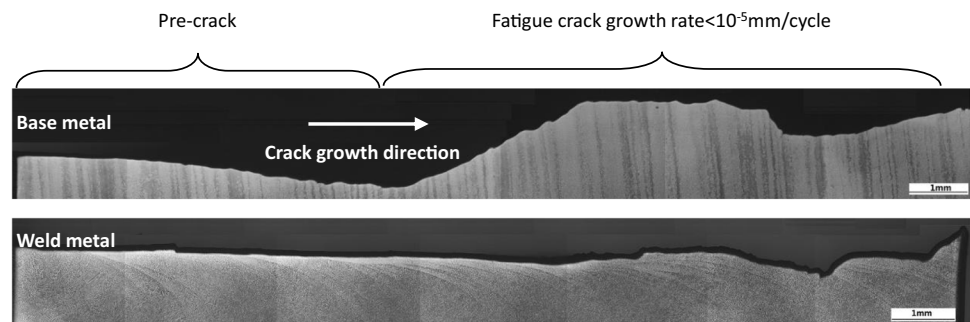


Fig. 10 Analysis of fatigue crack growth rate in near-threshold region ($< 10^{-5}$ mm/cycle)

crack growth rate less than 10^{-5} mm/cycle, the fatigue crack growth rate of weld metal with the stress ratio of 0.1 was slightly faster than that of base metal, while both of them were basically equal with the stress ratio of 0.5. Finally, under the worse case condition with the stress ratio of 0.9, the fatigue crack growth rate of weld metal was significantly lower than that of base metal, as shown in Fig. 10.

Figure 11 compares the morphology of near-threshold crack growth path (fatigue crack growth rate $< 10^{-5}$ mm/cycle) between weld metal and base metal under the condition of stress ratio of 0.1. Large deviations and fluctuations appeared in base metal during crack growth while deviation was very small in weld metal. Obviously, large

Fig. 11 Morphology of near-threshold crack growth path at $R=0.1$



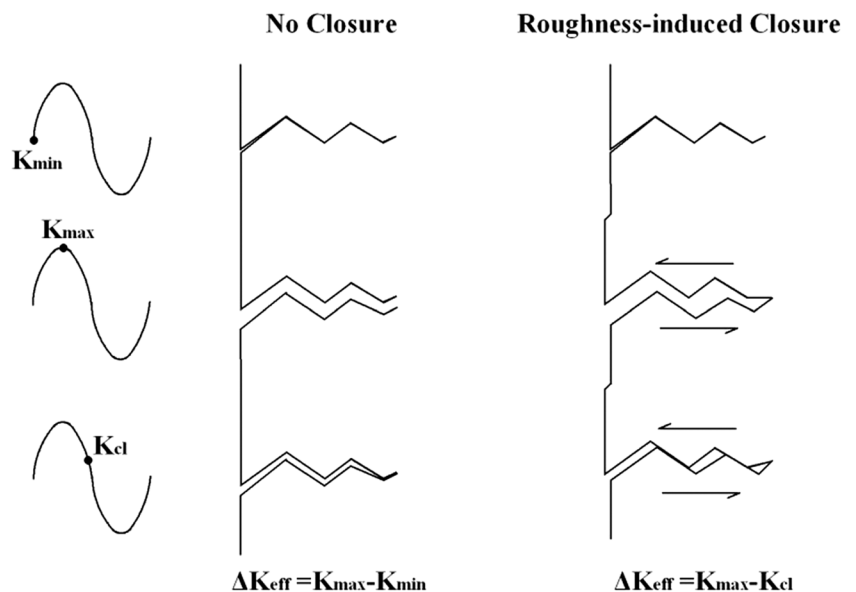
deviations and fluctuations along the crack growth path in base metal increased significantly the total length of crack growth, compared with weld metal.

3.4 Discussion

It is well known that significant roughness-induced crack closure can arise from an irregular or rough fracture surface morphology. Figure 12 shows the mechanism of roughness-induced crack closure, where the size scale of the fracture surface roughness is comparable with crack tip opening displacements and where significant Model II displacements exist (a situation found near-threshold levels at low stress ratios), crack closure again promoted since the crack may be wedged open at discrete contact points along the crack faces [19]. And the larger prior austenite grain size of metal material, the greater deviation and tortuosity of crack growth process, resulting in more serious surface roughness, and the greater the influence of crack closure effect, which will reduce near-threshold fatigue crack growth rate with low stress ratios [1 ~ 6]. Obviously, under the condition of low stress ratio of 0.1, the deviation and twists of near-threshold

crack path in base metal of 18Ni maraging steel were more serious than those in weld metal, as shown in Fig. 11, which was directly relative to the fact that the size of prior austenite grains in base metal of 18Ni maraging steel was larger than that of prior austenite dendrite in weld metal (the dendrite width is the main size characteristic that affects the behavior of crack transgranular growth), as shown in Fig. 4a and c. Accordingly, the discrepancy of rough fracture surface morphology caused by the difference of grain size between base metal and weld metal inevitably affected the difference of crack closure effect on near-threshold crack growth behavior under the condition of low stress ratio, as shown in Fig. 10. In addition, under the worse-case condition of stress ratio of 0.9, where crack closure effect has been completely eliminated, near-threshold crack growth rate of base metal was obviously faster than that of weld metal with very low ΔK -values, as shown in Fig. 11. However, under the condition of low stress ratio of 0.1, near-threshold crack growth rate of base metal was slightly lower than that of weld metal. Therefore, the significant change of crack growth behavior between base metal and weld metal under the extremely different loading conditions just proved that roughness-induced

Fig. 12 Schematic illustration of mechanism of roughness-induced crack. ΔK_{eff} is the effective stress intensity range, given by $K_{max} - K_{cl}$, where K_{max} is the Maximum stress intensity and K_{cl} is the stress intensity to close the crack; $K_{cl} \geq K_{min}$, the minimum stress intensity [19]



crack closure effect had a greater influence on crack growth behavior of base metal than that of weld metal under the condition of very low ΔK -values and low stress ratio.

Typically, crack closure effects disappear when the stress ratio is greater than 0.7 for metallic materials [20–22]. Under the worse-case condition of stress ratio of 0.9, where crack closure effect has been completely eliminated, weld metal has significant resistance of near-threshold crack growth, compared with base metal, as shown in Fig. 11. So, what role does the microstructure play in this phenomenon? According to the research results [13], block grain is the smallest microstructure unit that controls the properties of martensitic steel. Figure 13a and b shows the distribution of block grains in weld metal and base metal of 18Ni maraging steel, in which a color represents a single block grain with boundary of misorientation greater than 15°. Obviously, the average size of block grains of weld metal which is about 6.17 μm is significantly larger than that of base metal which is about 3.51 μm . In addition, Fig. 13c and d reveals various types of boundaries in weld metal and base metal. The statistical results of the number and length of various types of boundaries in weld metal and base metal are displayed in Fig. 14. Regardless of high-angle boundaries with misorientation greater than 15° or low-angle boundaries with

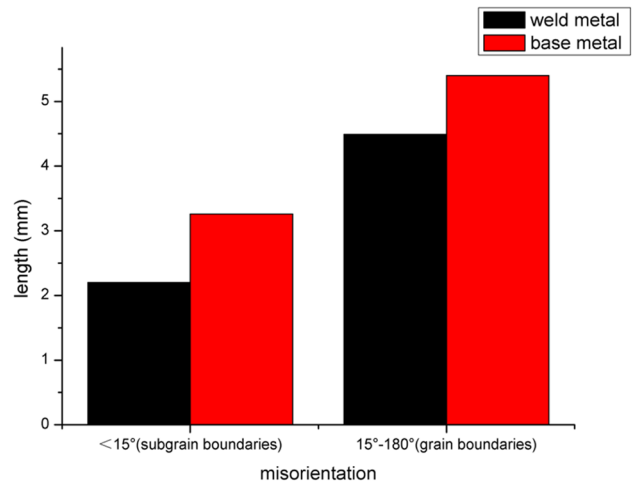
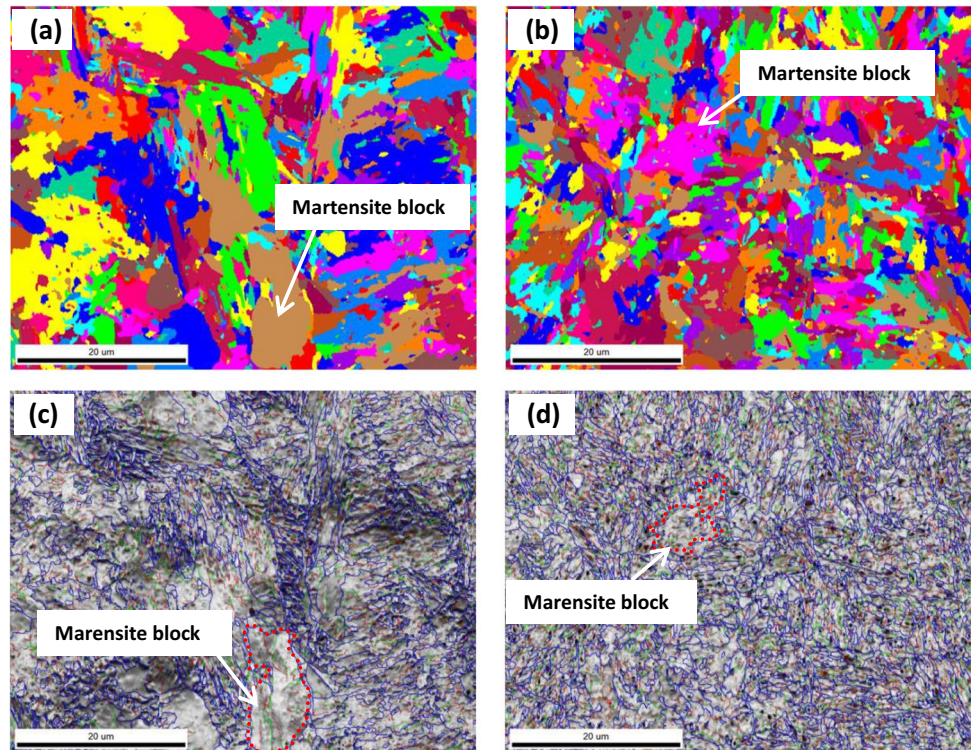


Fig. 14 Total length of grain boundaries and subgrain boundaries of weld metal and base metal

misorientation less than 15°, the quantity and total length in weld metal are obviously smaller than those of base metal. Correspondingly, it can also be inferred that the densities of high-angle boundaries and low-angle boundaries in weld metal are necessarily less than those in base metal.

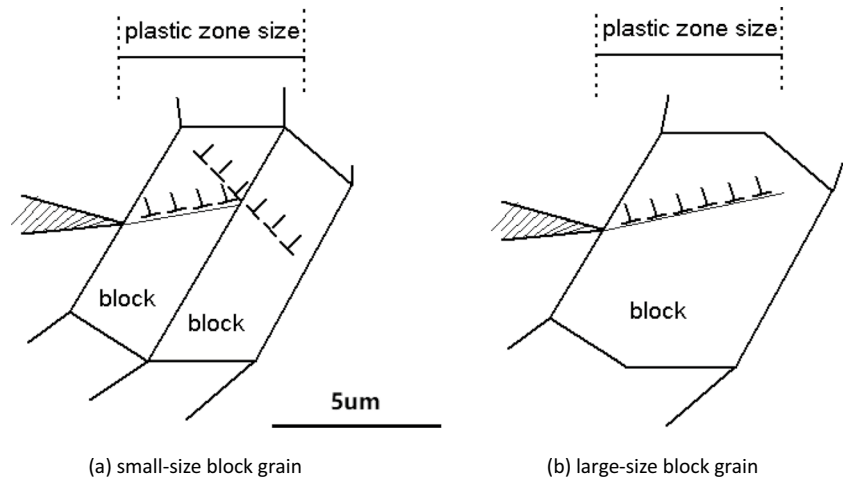
Fig. 13 EBSD test results of microstructure of weld metal and base metal. a Grain morphology of weld metal. b Grain morphology of base metal. c Grain boundary orientation of weld metal. d Grain boundary orientation of base metal



Boundaries: Rotation Angle

| | Min | Max |
|-------|-----|------|
| Red | 2° | 5° |
| Green | 5° | 15° |
| Blue | 15° | 180° |

Fig. 15 Schematic diagram of dislocation structure in front of the crack tip



As stress ratio R increases, mean stress increases, and when the stress ratio $R=0.9$, the plastic zone at the crack tip is close to the unidirectional plastic zone. Figure 15 shows schematically the crack tip state of small-size and large-size martensite block grains. In order to explain the different near-threshold stress intensity values for two types of block grains, a situation will be considered where the plastic zone size at peak load should be somewhat smaller than the large block grain size, as shown in Fig. 15b. At very low ΔK -values, where in an idealized case only one slip system may be activated, pile-up dislocations are formed in the same slip plane in front of the crack tip in large-size block grain. However, in small-size block grain, dislocations plugging will occur at the grain boundary in front of the crack tip, and high local stress concentration will lead to slip on the secondary slip system in the same grain and slip in adjacent grains, as shown in Fig. 15a. Obviously, compared with weld metal, base metal with smaller block grain size and higher density of high-angle boundaries will form more dislocations plugging during the loading process, so that the extra stress at the crack tip in base metal is greater than that in weld metal, thereby increasing the effective stress intensity value of near-threshold crack growth, which explains the crack growth rate of base metal is faster than that of weld metal under the condition of $R=0.9$. However, at lower stress ratios, $R=0.1$, microstructure of block grain is insensitive to the influence of fatigue crack growth rate due to the crack closure effect.

In addition, according to the research result of Reference [23], existence of retained austenite phase in metal materials was beneficial to increase near-threshold crack growth resistance. Obviously, this is relative to the fact that the plastic deformation formed by the low-strength, well-plasticized austenite at the crack tip consumes the energy required for crack growth. According to the statistical results of austenite phases shown in Fig. 8, the amount of retained and reversed

austenite phases in weld metal were much larger than that of base metal, which may also be an important factor to increase the near-threshold crack growth resistance.

4 Conclusion

- (1) The total amount of retained austenite phase and reversed austenite phase in weld metal was 5 times more than that in base metal, which consumes consequently more elements such as Mo, Ti, and Ni in the matrix of weld metal, and which will inevitably have negative influences on the mechanical properties of weld metal.
- (2) When fatigue crack growth rate is less than 10^{-5} mm/cycle at the stress ratio of 0.1, roughness-induced crack closure has a greater influence on crack growth behavior of base metal than that of weld metal.
- (3) When fatigue crack growth rate is less than 10^{-5} mm/cycle at the stress ratio of 0.9, fatigue crack in base metal with smaller block grain size and higher density of high-angle boundaries grows faster than weld metal with larger block grain size.

Declarations

Conflict of interest The authors declare no competing interests.

References

1. Newman JA (2000) The effects of load ratio on threshold fatigue crack growth of aluminum alloys [D]. Virginia Polytechnic Institute and State University, Blacksburg, Virginia, USA

2. Petit J, Sarrazin-Baudoux C (2010) Some critical aspects of low rate fatigue crack propagation in metallic materials [J]. *Int J Fatigue* 32(6):962–970
3. Nani Babu M, Shashank Dutt B, Venugopal S et al (2010) On the anomalous temperature dependency of fatigue crack growth of SS 316(N) weld [J]. *Mater Sci Eng A* 527:5122–5129
4. Ritchie RO (1977) Influence of microstructure on near-threshold fatigue-crack propagation in ultra-high strength steel [J]. *Metal Sci* 11(8-9):369–381
5. Sun Q, Li K, Li X et al (2020) Near-threshold fatigue crack growth behavior of 10% Cr martensitic steel welded joint with 9% Cr welded joint with 9% Cr weld metal in high temperature air [J]. *Int J Fatigue* 131:1–11
6. Gray GT III, Williams JC, Thompson AW (1983) Roughness-induced crack closure: an explanation for microstructurally sensitive fatigue crack growth [J]. *Metall Trans A* 14A:421–433
7. Sun L, Cai Z et al (2014) Study on influence of prior austenite size on critical point between stable and near-threshold fatigue crack propagation in weld metal of a nuclear turbine rotor [J]. *China Mech Eng* 25(24):3378–3384
8. Yoder GR, Cooley LA, Crooker TW (1983) The effect of load ratio on fatigue crack growth in Ti-8Al-1Mo-1V. *Engng Fract Mech* 17:185–188
9. da Fonte M, Romeiro F, de Freitas M, Stanzl-Tschegg SE, Tschegg EK, Vasudevan AK (2003) The effect of microstructure and environment on fatigue crack growth in 7049 aluminium alloy at negative stress ratios [J]. *Int J Fatigue* 25:1209–1216
10. Oberwinkler B (2011) Modeling the fatigue crack growth behavior of Ti-6Al-4V by considering grain size and stress ratio [J]. *Mater Sci Engng A* 528:5983–5992
11. Shademan S, Sinha V, Soboyejo ABO, Soboyejo WO (2004) An investigation of the effects of microstructure and stress ratio on fatigue crack growth in Ti- 6Al-4V with colony alpha/beta microstructures [J]. *Mech Mater* 36:161–175
12. Jha SK, Ravichandran KS (2000) Effect of mean stress (stress ratio) and aging on fatigue-crack growth in a metastable beta titanium alloy, Ti-10V-2Fe-3Al J. *Metall Mater Trans A* 31:703–714
13. Yang M, Zhang Y, Liang Y-l (2018) Effect of hierarchical microstructures of lath martensite on the transitional behavior of fatigue crack growth rate [J]. *Met Mater Int* 24:970–980
14. Wang B, Zhang P et al (2017) Optimizing the fatigue strength of 18Ni maraging steel through ageing treatment [J]. *Mater Sci Eng A* 707:674–688
15. He Y, Liu K, Yang K (2003) Effect of solution temperature on fracture toughness and microstructure of ultra-purified 18Ni (350) maraging steel [J]. *Acta Metall Sin* 39(4):381–386
16. Wei C, Xiaoying H, Tianxi P et al (1981) Effects of the microstructure of weld metal on the fracture toughness of 18Ni (250) maraging steel [J]. *Iron Steel* 16(1):42–46
17. Chen J-g, Zhang J-f et al (2009) Outline of strengthening ways in 18Ni maraging steel[J]. *Met Funct Mater* 16(4):46–49
18. Huang X, Chen W (1981) Inversely transformed austenite formed during welding of 18Ni (250 grade) maraging steels[J]. *Iron Steel* 2:60–61
19. Ritchie RO, Suresh S (1982) Some considerations on fatigue crack closure at near-threshold stress intensities due to fracture surface morphology [J]. *Metall Transactions A* 13A:937–940
20. Tsukuda H, Ogiyama H, Shiraishi T (1995) Fatigue crack growth and closure at high stress ratios [J]. *Fatigue Fract Engng Mater Struct* 18:503–514
21. Mishra MP, Packiaraj CC, Ray SK, Mannan SL, Borgstedt HU (1997) Influence of sodium environment and load ratio (R) on fatigue crack growth behaviour of a type 316 LN stainless steel at 813 K [J]. *Int J Pres Ves Pip* 70:77–82
22. Ding J, Hall R, Byrne J (2005) Effects of stress ratio and temperature on fatigue crack growth in a Ti-6Al-4V alloy [J]. *Int J Fatigue* 27:1551–1558
23. Ritchie RO, Chang VA, Paton NE (1979) Influence of retained austenite on fatigue crack propagation in HP9-4-20 high strength alloy steel [J]. *Fatigue of Eng Mater Struct* 1:107–121

Publisher's Note Springer Nature remains neutral with regard to jurisdictional claims in published maps and institutional affiliations.

Springer Nature or its licensor (e.g. a society or other partner) holds exclusive rights to this article under a publishing agreement with the author(s) or other rightsholder(s); author self-archiving of the accepted manuscript version of this article is solely governed by the terms of such publishing agreement and applicable law.